

# Phase diagram of strong matter at finite chemical potentials

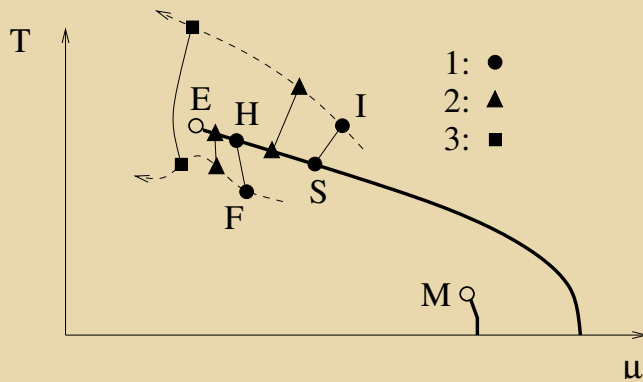
Péter Kovács

KFKI Research Inst. of Part. and Nucl. Phys. of HAS, Theoretical Department

Hévíz, jan. 23 - 25, 2008

- Motivation for investigating QCD at non-zero  $\mu_I, \mu_Y$
- The constituent quark model and its parameterization
- Introduction of the chemical potentials:  $\mu_B, \mu_I, \mu_Y$
- Results at  $\mu_I = \mu_Y = 0$
- Results at non-zero  $\mu_I, \mu_Y$
- Conclusions

# Relevance of the isospin and strange chemical potentials



- the CEP is experimentally accessible
- $\mu_B, \mu_I \neq 0$  in heavy ion collision experiments
- $\mu_B$  is tunable  $\rightarrow$  beam energy, centrality
- $\mu_I$  is tunable  $\rightarrow$  different isotopes of an element
- In some experiment even  $\mu_Y$  plays role
- Focusing effect: if CEP exist it cannot be missed

Brookhaven AGS exp. Si+Au collision: at  $\mu_B = 540 \text{ MeV} \rightarrow \mu_Y \approx 150 \text{ MeV}$

CERN SPS exp. Pb+Pb collision:  
at  $\mu_B = 233 - 266 \text{ MeV} \rightarrow \mu_Y \approx 70 - 80 \text{ MeV}, \mu_I \approx 12 - 13 \text{ MeV}$

CMB exp. at FAIR will explore QCD phase diagram at high  $\mu_B$

Analogy to the QCD CEP  $\rightarrow$  liquid-gas phase transition which is easy to hit

lattice simulations at finite chemical potential is very difficult

$\implies$  not all the methods predict/find the CEP

CEP found at:  $(T, \mu_B)_{\text{CEP}} = (162 \pm 2, 360 \pm 40) \text{ MeV}$ , volume:  $12 \times 4^3$  and  $m_\pi = m_\pi^{\text{phys}}$

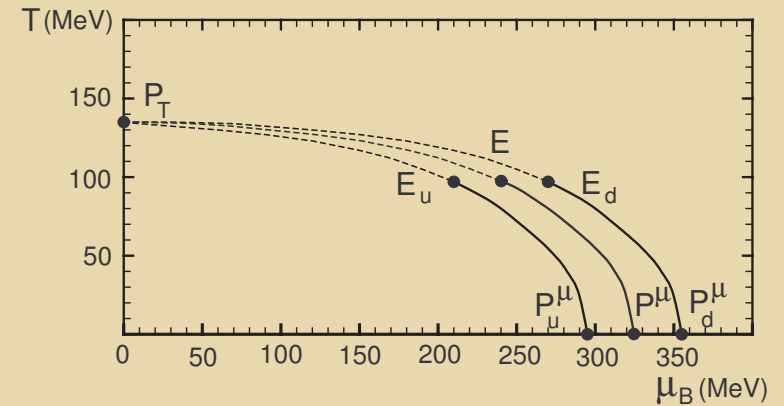
Z. Fodor, S. D. Katz, JHEP 0404:050,2004

it is important to study the CEP and its  $\mu_I, \mu_Y$  dependence in effective models

# Influence of $\mu_I$ on the $\mu_B - T$ diagram

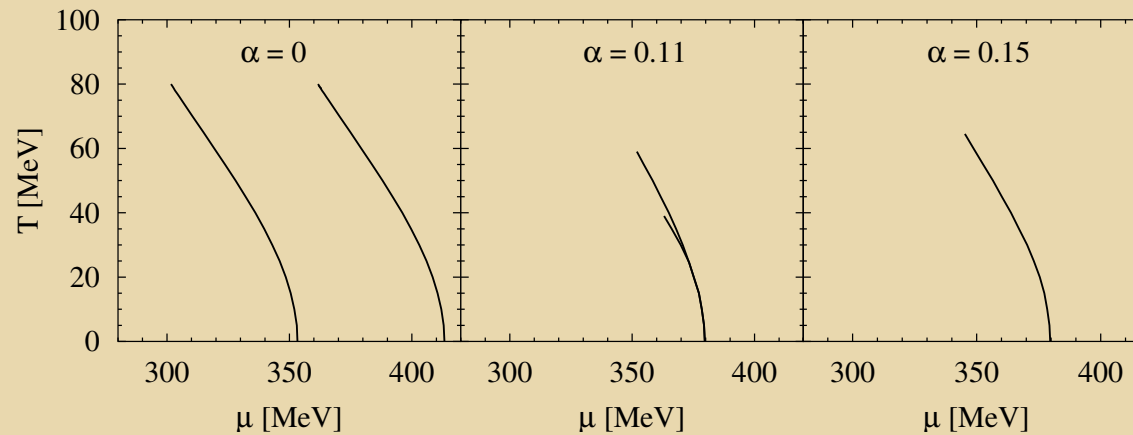
Barducci et. al, PLB **564**, 217

without  $U(1)_A$  breaking  $\rightarrow$  generic result  
for low  $T$   $\mu_I$  induces two 1<sup>st</sup> order transitions  
 $\implies$  2 critical endpoints



the structure **cease to exist** in case of a sufficiently strong  $U(1)_A$  breaking

Frank et. al, PLB **562**, 221



## $SU_L(3) \times SU_R(3)$ symmetric chiral quark model

$$\mathcal{L} = \frac{1}{2} \text{Tr}(\partial_\mu M^\dagger \partial^\mu M + m_0^2 M^\dagger M) - f_1 (\text{Tr}(M^\dagger M))^2 - f_2 \text{Tr}(M^\dagger M)^2 \\ - g (\det(M) + \det(M^\dagger)) + \epsilon_0 \sigma_0 + \epsilon_3 \sigma_3 + \epsilon_8 \sigma_8 + \bar{\psi} (i \not{\partial} - g_F M_5) \psi.$$

$$M = \frac{1}{\sqrt{2}} \sum_{i=0}^8 (\sigma_i + i \pi_i) \lambda_i, \quad M_5 = \sum_{i=0}^8 \frac{1}{2} (\sigma_i + i \gamma_5 \pi_i) \lambda_i \quad 3 \times 3 \text{ complex matrices}$$

pseudo(**scalar**) fields:  $\pi_i, \sigma_i$ , constituent quark field:  $\bar{\psi} = (u, d, s)$

Gell-Mann matrices:  $\lambda_0 := \sqrt{\frac{2}{3}} \mathbf{1}$ ,  $\lambda_i : i = 1 \dots 8$ .

**determinant** breaks  $U_A(1)$  symmetry

**explicit symmetry breaking**: external fields  $\epsilon_0, \epsilon_3, \epsilon_8 \neq 0 \iff m_u \neq m_d \neq 0, m_s \neq 0$

broken symmetry phase: three condensates  $(\langle \sigma_0 \rangle, \langle \sigma_8 \rangle), \langle \sigma_3 \rangle \longleftrightarrow (x, y), v_3$

x: non-strange, y: strange

$$\text{fermion masses: } M_u = \frac{g_F}{2} (x + v_3), \quad M_d = \frac{g_F}{2} (x - v_3), \quad M_s = \frac{g_F y}{\sqrt{2}}$$

technical difficulty: mixing in the 0, 3, 8 sector

parameters determined from the  $T = 0$  mass spectrum

# Parameterization and thermodynamics at one-loop level

13 unknown parameters:

couplings	$m_0^2, f_1, f_2, g, g_F$
condensates	$x, y, v_3$
external fields	$\epsilon_x, \epsilon_y, \epsilon_3$
renormalization scales	$l_f, l_b$

resummation using optimized perturbation theory Chiku & Hatsuda, PRD58:076001

change:  $-m_0^2 \rightarrow m^2 \Rightarrow \mathcal{L}_{mass} = \frac{1}{2}m^2 \text{Tr} M^\dagger M - \frac{1}{2} \underbrace{(m_0^2 + m^2) \text{Tr} M^\dagger M}_{\Delta m^2: \text{one-loop counterterm}}$

fastest apparent convergence  $M_\pi^2 = iG^{-1}(p^2=0)|_{1\text{-loop}} \stackrel{!}{=} m_\pi^2|_{\text{tree}} \implies$  equation for the effective mass:

$$m^2 = -m_0^2 + \Sigma_\pi(p=0, m_i(m^2), M_q)$$

From the tree-level pion mass:  $m^2 = m_\pi^2 - (4f_1 + 2f_2)x^2 - 4f_1y^2 - 2gy$

$\implies$  introducing into the other tree-level masses

$\implies$  self-consistent gap equation for the pion mass

## Set of coupled nonlinear equations (for $v_3 = 0$ ):

(1) gap-equation:  $m_\pi^2 = -m_0^2 + (4f_1 + 2f_2)x^2 + 4f_1y^2 + 2gy + \text{Re}\Sigma_\pi(p=0, m_i(m_\pi), M_u)$

(2) pole-mass  $M_K$  from:

$$M_K^2 = -m_0^2 + 2(2f_1 + f_2)(x^2 + y^2) + 2f_2y^2 - \sqrt{2}x(2f_2y - g) + \text{Re}\Sigma_K(p^2 = M_K^2, m_i)$$

(3) FAC criterion for  $M_K$ :  $\Sigma(p^2 = M_K^2) = 0$

(4) pole-mass  $M_\eta$  from:

$$\text{Det} \begin{pmatrix} p^2 - m_{\eta xx}^2 - \Sigma_{\eta xx}(p^2, m_i) & -m_{\eta xy}^2 - \Sigma_{\eta xy}(p^2, m_i) \\ -m_{\eta xy}^2 - \Sigma_{\eta xy}(p^2, m_i) & p^2 - m_{\eta yy}^2 - \Sigma_{\eta yy}(p^2, m_i) \end{pmatrix} \Big|_{p^2=M_\eta^2, M_{\eta'}} = 0$$

(5) tree-level PCAC:  $x = f_\pi$

(6) From non-strange quark mass:  $g_F = \frac{2M_u}{x}$

(7) From strange quark mass:  $y = \frac{\sqrt{2}M_s}{g_F}$

(8) EOS for x:

$$\epsilon_x = -m_0^2x + 2gxy + 4f_1xy^2 + 2(2f_1 + f_2)x^3 + \sum_{\alpha,i,j} t_{\alpha,i,j}^x \langle \alpha_i \alpha_j \rangle + \frac{g_F}{2} (\langle \bar{u}u \rangle + \langle \bar{d}d \rangle)$$

(9) EOS for y:  $\epsilon_y = -m_0^2y + gx^2 + 4f_1x^2y + 4(f_1 + f_2)y^3 + \sum_{\alpha,i,j} t_{\alpha,i,j}^y \langle \alpha_i \alpha_j \rangle + \frac{g_F}{\sqrt{2}} \langle \bar{s}s \rangle$

## Differences in case of isospin breaking

New variable:  $v_3$

Equation for  $v_3 \longrightarrow$  third EoS:

$$\left\langle \frac{\partial \mathcal{L}}{\partial \sigma_3} \right\rangle = 0 \quad (1)$$

Even if  $\epsilon_3 = 0$  ( $\implies v_3 = 0$  at  $T = 0$ ) non zero  $\mu_I$  will generate  $v_3$  at non zero temperature

**Consequence:** charged and neutral particle masses will be different at tree level

If explicit isospin breaking is also introduced another equation is needed:

$$m_{\pi^+, \text{tree}} - m_{\pi^0, \text{tree}} = 4.594 \text{MeV} \quad (2)$$

This equation will determine  $v_3$  at  $T = 0$  and EoS for  $v_3$  at  $T = 0$  will determine  $\epsilon_3$

# Introduction of chemical potentials

21 particles:

pseudoscalars	$\pi^0, \eta, \eta', \pi^+, \pi^-, K^+, K^-, K^0, \bar{K}^0$
scalars	$\sigma, a_0^0, f_0, a_0^+, a_0^-, \kappa^+, \kappa^-, \kappa^0, \bar{\kappa}^0$
fermions	$m_u, m_d, m_s$

Lagrangian is invariant under

$$M \rightarrow e^{-i\alpha_G G} M e^{i\alpha_G G} = M - i\alpha_G [G, M] + \mathcal{O}(\alpha_G^2),$$

$$\psi \rightarrow e^{-i\alpha_G G} \psi = \psi - i\alpha_G \psi + \mathcal{O}(\alpha_G^2),$$

where  $G$  can be  $B = \sqrt{\frac{3}{2}}\lambda_0$ ,  $I = \frac{1}{2}\lambda_3$  and  $Y = \frac{1}{\sqrt{3}}\lambda_8$

The conserved Noether currents:

$$J_\mu^G = -\frac{\delta L}{\delta(\partial^\mu M)_{ij}} i[G, M]_{j,i} - \frac{\delta L}{\delta(\partial^\mu M^+)_{ij}} i[G, M^+]_{j,i} - \frac{\delta L}{\delta(\partial^\mu \psi_i)} iG_{ij} \psi_j$$



The conserved charges:

$$Q^B = \frac{1}{3}(N_u + N_d + N_s - N_{\bar{u}} - N_{\bar{d}} - N_{\bar{s}}),$$

$$Q^I = \frac{1}{2}(N_u - N_{\bar{u}} - N_d + N_{\bar{d}} + N_{\kappa^+} - N_{\kappa^-} + N_{\bar{\kappa}^0} - N_{\kappa^0} + N_{K^+} - N_{K^-} + N_{\bar{K}^0} - N_{K^0}) \\ + N_{a_0^+} - N_{a_0^-} + N_{\pi^+} - N_{\pi^-},$$

$$Q^Y = \frac{1}{3}(N_u - N_{\bar{u}} + N_d - N_{\bar{d}} - 2N_s + 2N_{\bar{s}}) + N_{\kappa^+} - N_{\kappa^-} + N_{\kappa^0} - N_{\bar{\kappa}^0} + N_{K^+} - N_{K^-} + N_{K^0} - N_{\bar{K}^0}$$

Statistical density matrix of the system:

$$\rho = \exp[-\beta(H - \mu_i N_i)]$$

The following chemical potentials can be introduced:

$$\mu_u = -\mu_{\bar{u}} = \frac{1}{3}\mu_B + \frac{1}{2}\mu_I + \frac{1}{3}\mu_Y,$$

$$\mu_d = -\mu_{\bar{d}} = \frac{1}{3}\mu_B - \frac{1}{2}\mu_I + \frac{1}{3}\mu_Y,$$

$$\mu_s = -\mu_{\bar{s}} = \frac{1}{3}\mu_B - \frac{2}{3}\mu_Y,$$

$$\mu_{a_0^+} = \mu_{\pi^+} = -\mu_{a_0^-} = -\mu_{\pi^-} = \mu_I,$$

$$\mu_{\kappa^+} = \mu_{K^+} = -\mu_{\kappa^-} = -\mu_{K^-} = \frac{1}{2}\mu_I + \mu_Y,$$

$$\mu_{\kappa^0} = \mu_{K^0} = -\mu_{\bar{\kappa}^0} = -\mu_{\bar{K}^0} = -\frac{1}{2}\mu_I + \mu_Y$$

# Finite temperature propagators of charged fields

For example the  $K^-$ ,  $K^+$  field operators:

$$K^-(x) = \int \frac{d^3\mathbf{p}}{(2\pi)^3} \frac{1}{\sqrt{2E_{\mathbf{p}}}} \left( a^+(\mathbf{p})e^{ip \cdot x} + b(\mathbf{p})e^{-ip \cdot x} \right) \Big|_{p_0=E_{\mathbf{p}}},$$

$$K^+(x) = \int \frac{d^3\mathbf{p}}{(2\pi)^3} \frac{1}{\sqrt{2E_{\mathbf{p}}}} \left( b^+(\mathbf{p})e^{ip \cdot x} + a(\mathbf{p})e^{-ip \cdot x} \right) \Big|_{p_0=E_{\mathbf{p}}}$$

The two-point functions:

$$G_{K^-}(y-x) := \langle TK^-(y)K^+(x) \rangle_{\beta} = \Theta(y_0 - x_0) \langle K^-(y)K^+(x) \rangle_{\beta} + \Theta(x_0 - y_0) \langle K^+(x)K^-(y) \rangle_{\beta},$$

$$G_{K^+}(y-x) := \langle TK^+(y)K^-(x) \rangle_{\beta} = \Theta(y_0 - x_0) \langle K^+(y)K^-(x) \rangle_{\beta} + \Theta(x_0 - y_0) \langle K^-(x)K^+(y) \rangle_{\beta},$$

In momentum space the finite temperature propagators:

$$G_{K^-}(k) = \frac{i}{2E_{\mathbf{k}}} \left[ \frac{1 + n_{K^-}(E_{\mathbf{k}})}{k_0 - E_{\mathbf{k}} + i\epsilon} - \frac{n_{K^-}(E_{\mathbf{k}})}{k_0 - E_{\mathbf{k}} - i\epsilon} - \frac{1 + n_{K^+}(E_{\mathbf{k}})}{k_0 + E_{\mathbf{k}} - i\epsilon} + \frac{n_{K^+}(E_{\mathbf{k}})}{k_0 + E_{\mathbf{k}} + i\epsilon} \right]$$

$$G_{K^+}(k) = \frac{i}{2E_{\mathbf{k}}} \left[ \frac{1 + n_{K^+}(E_{\mathbf{k}})}{k_0 - E_{\mathbf{k}} + i\epsilon} - \frac{n_{K^+}(E_{\mathbf{k}})}{k_0 - E_{\mathbf{k}} - i\epsilon} - \frac{1 + n_{K^-}(E_{\mathbf{k}})}{k_0 + E_{\mathbf{k}} - i\epsilon} + \frac{n_{K^-}(E_{\mathbf{k}})}{k_0 + E_{\mathbf{k}} + i\epsilon} \right]$$

# Self-energies

$$-i\Sigma_{\pi^+} = \sum_{\substack{f \in (\sigma, \pi) \\ \alpha=0 \dots 8}} \text{Diagram 1} + \sum_{\delta=0,3,8} \text{Diagram 2} + \text{Diagram 3} + \text{Diagram 4} + \sum_{\delta=0,3,8} \text{Diagram 5} + \text{Diagram 6}$$

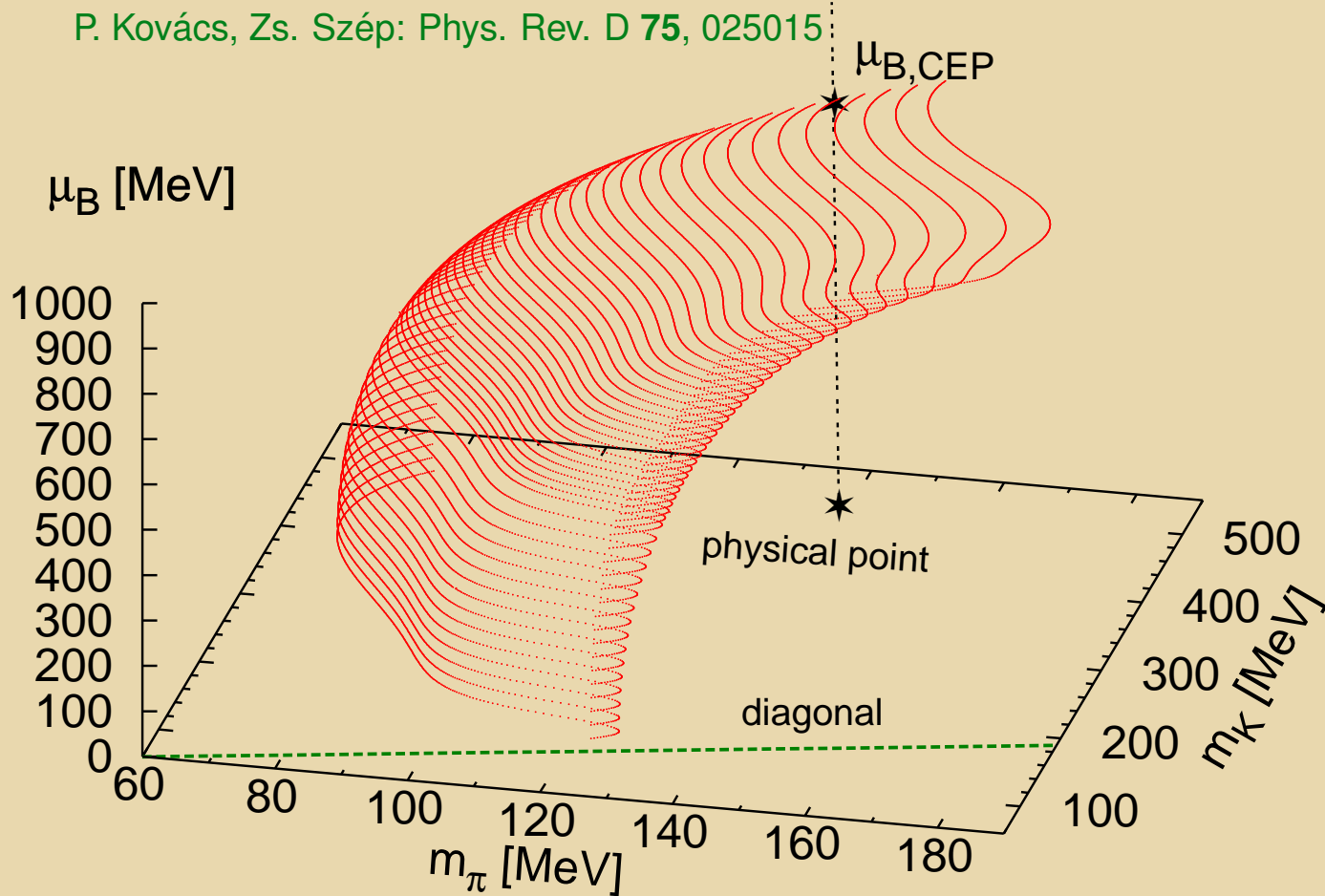
$$-i\Sigma_{0,3,8}^{\gamma\gamma'} = \sum_{\substack{f \in (\sigma, \pi) \\ \alpha=0 \dots 8}} \text{Diagram 1} + \sum_{\delta=0,3,8} \text{Diagram 2} + \text{Diagram 3} + \text{Diagram 4} + \text{Diagram 5} + \text{Diagram 6}$$

$$+ \text{Diagram 1} + \sum_{\delta, \delta'=0,3,8} \text{Diagram 2} + \sum_{q=u,d,s} \text{Diagram 3}$$

$$-i\Sigma_{K^+} = \sum_{\substack{f \in (\sigma, \pi) \\ \alpha=0 \dots 8}} \text{Diagram 1} + \text{Diagram 2} + \sum_{\delta=0,3,8} \text{Diagram 3} + \text{Diagram 4} + \sum_{\delta=0,3,8} \text{Diagram 5} + \text{Diagram 6}$$

# Results at zero $\mu_I, \mu_Y$ : critical surface and CEP

P. Kovács, Zs. Szép: Phys. Rev. D **75**, 025015

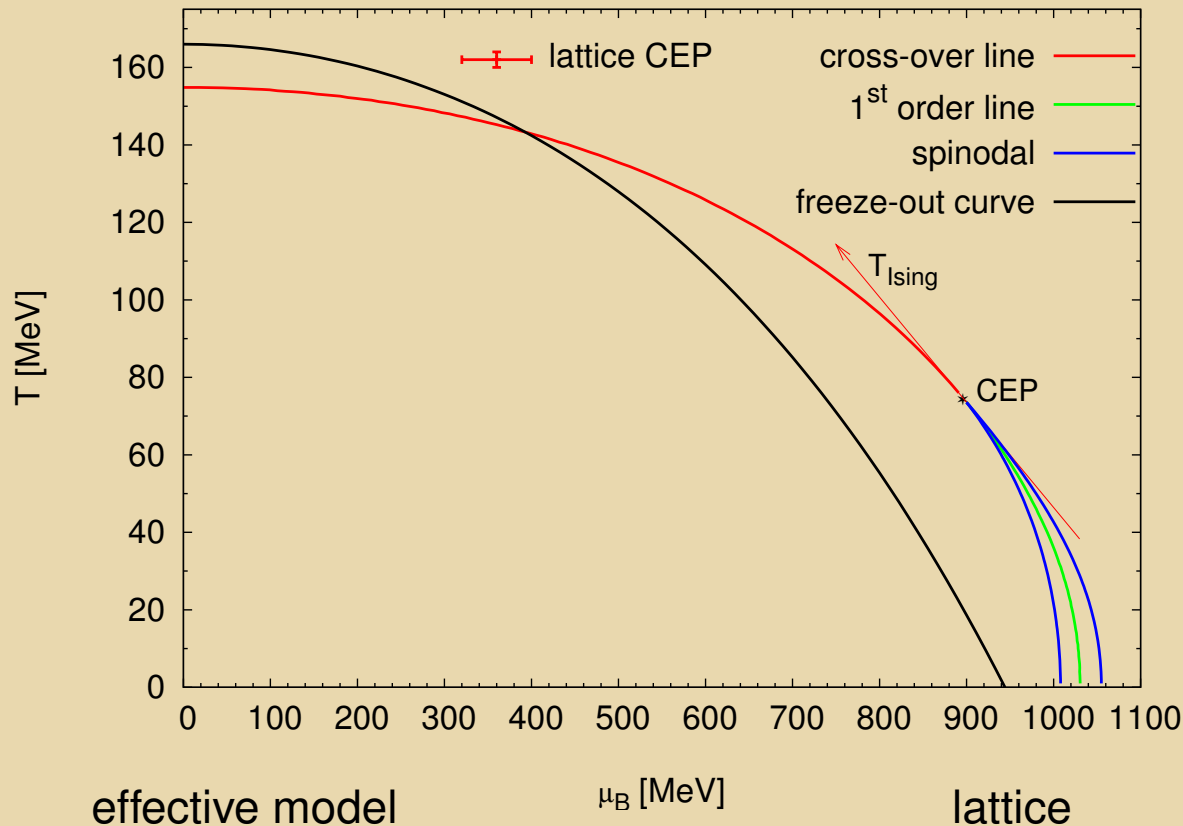


The surface bends towards the physical point  $\implies$  **The CEP must exist**

The continuation is reliable up to  $m_K \approx 500$  MeV and above the diagonal

# The CEP at the physical point of the mass plane

P. Kovács, Zs. Szép: Phys. Rev. D **75**, 025015



- $T_c(\mu_B = 0) = 154.84 \text{ MeV}$   
 $\Delta T_c(x\chi) = 15.5 \text{ MeV}$

- $T_{CEP} = 74.83 \text{ MeV}$   
 $\mu_{B,CEP} = 895.38 \text{ MeV}$

- $T_c \left. \frac{d^2 T_c}{d\mu_B^2} \right|_{\mu_B=0} = -0.09$

- $T_c(\mu_B = 0) = 151(3) \text{ MeV}$   
 $\Delta T_c(\chi_{\bar{\psi}\psi}) = 28(5) \text{ MeV}$

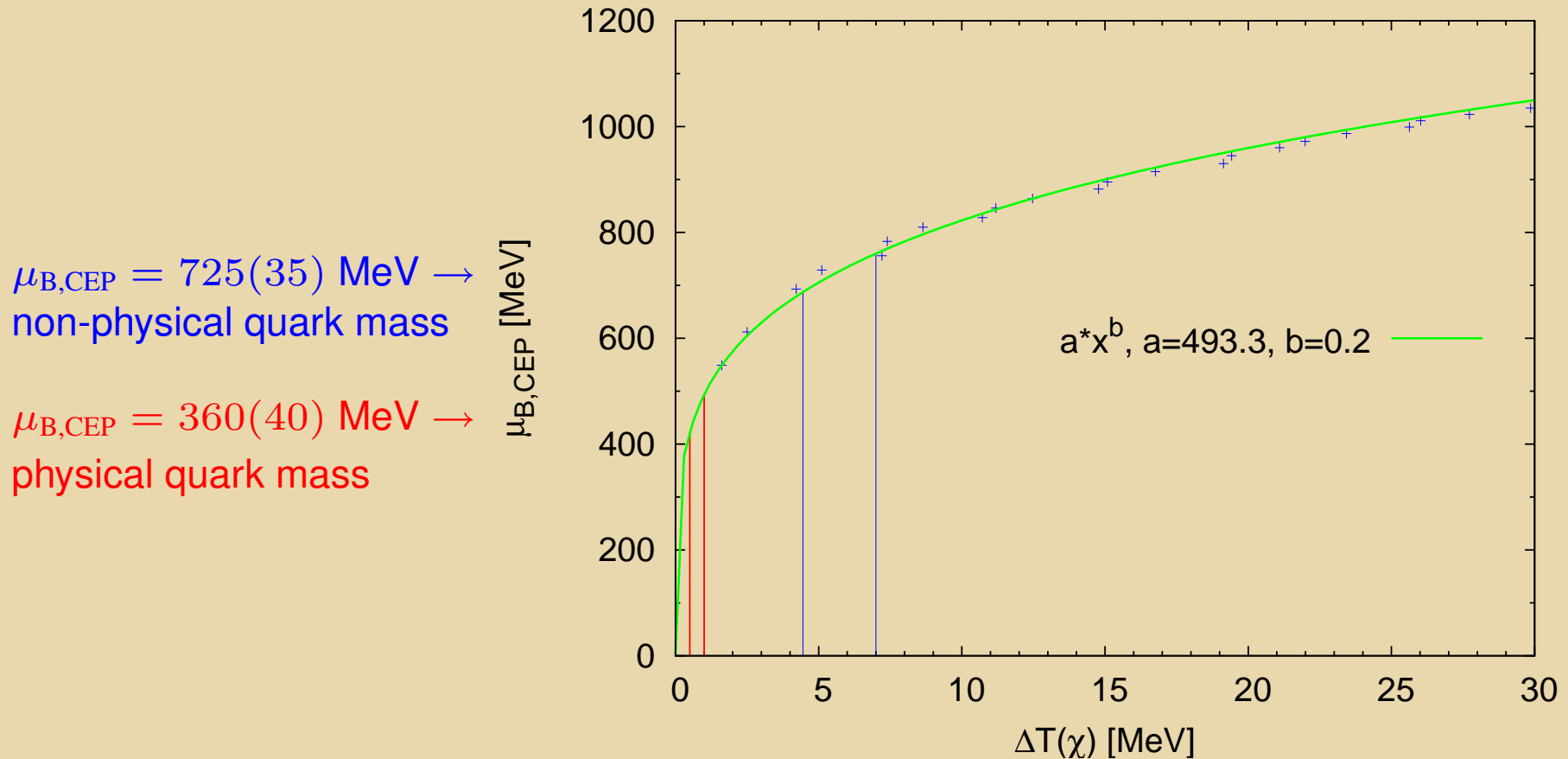
Y. Aoki, *et al.*, PLB **643**, 46 (2006)

- $T_{CEP} = 162(2) \text{ MeV}$   
 $\mu_{B,CEP} = 360(40) \text{ MeV}$

- $-0.058(2)$

Z. Fodor, *et al.*, JHEP 0404 (2004) 050

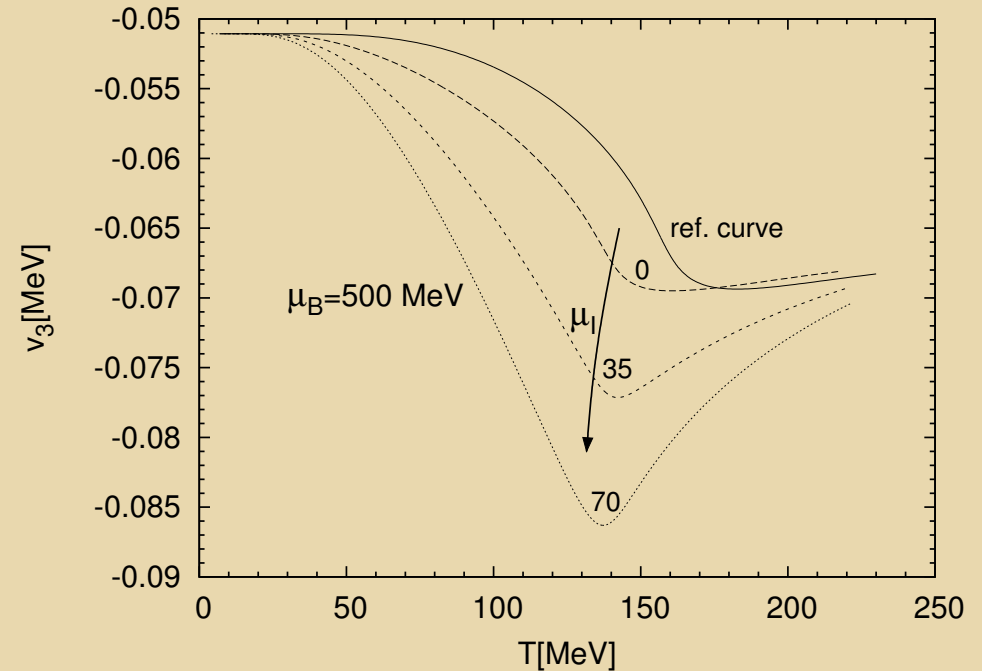
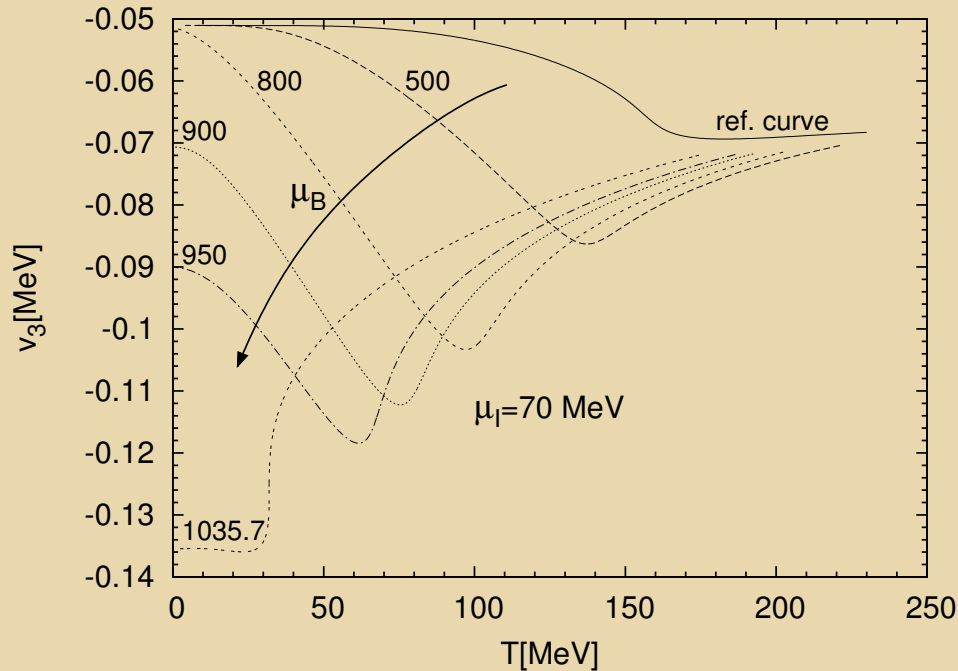
# Dependence of the $\mu_{B,CEP}$ on the width of the susceptibility



Preliminary lattice estimation by S. Katz:  $\Delta T_c(\chi_{\bar{\psi}\psi}) \approx 0.5 - 1 \text{ MeV}$   
 $\Delta T_c(\chi_{\bar{\psi}\psi}) \approx 2 - 4 \text{ MeV}$

Since  $\Delta T_c(\chi_{\bar{\psi}\psi}) \approx 28 \text{ MeV}$  at the physical point  $\longrightarrow$  higher  $\mu_{B,CEP}$  expected

## Temperature dependence of $v_3$



On the left Fig.:  $\mu_B$  dependence at a given  $\mu_I$   
 Lowest curve corresponds to a CEP

$v_3$  at  $T = 0$  significantly depend on  $\mu_B$

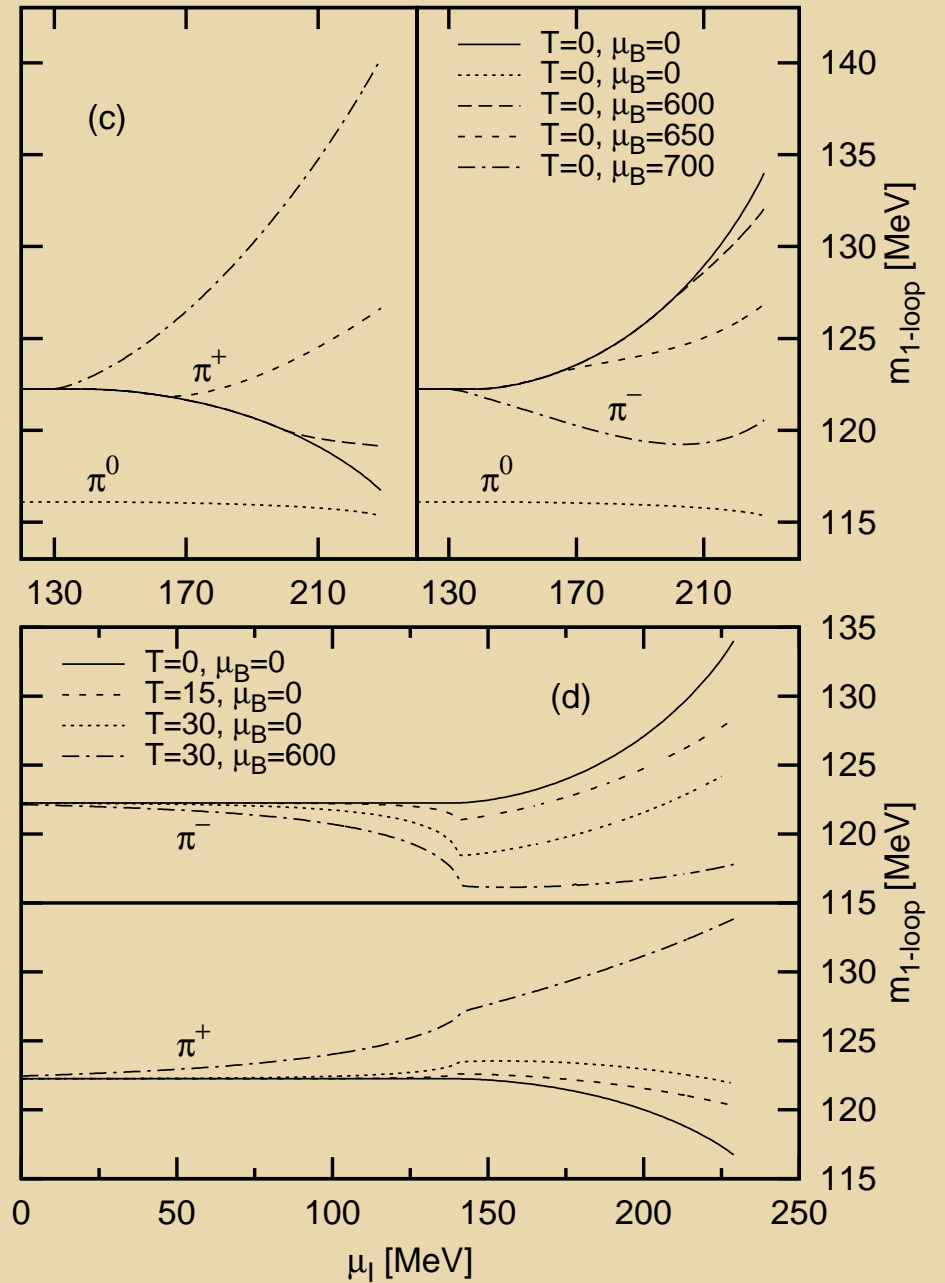
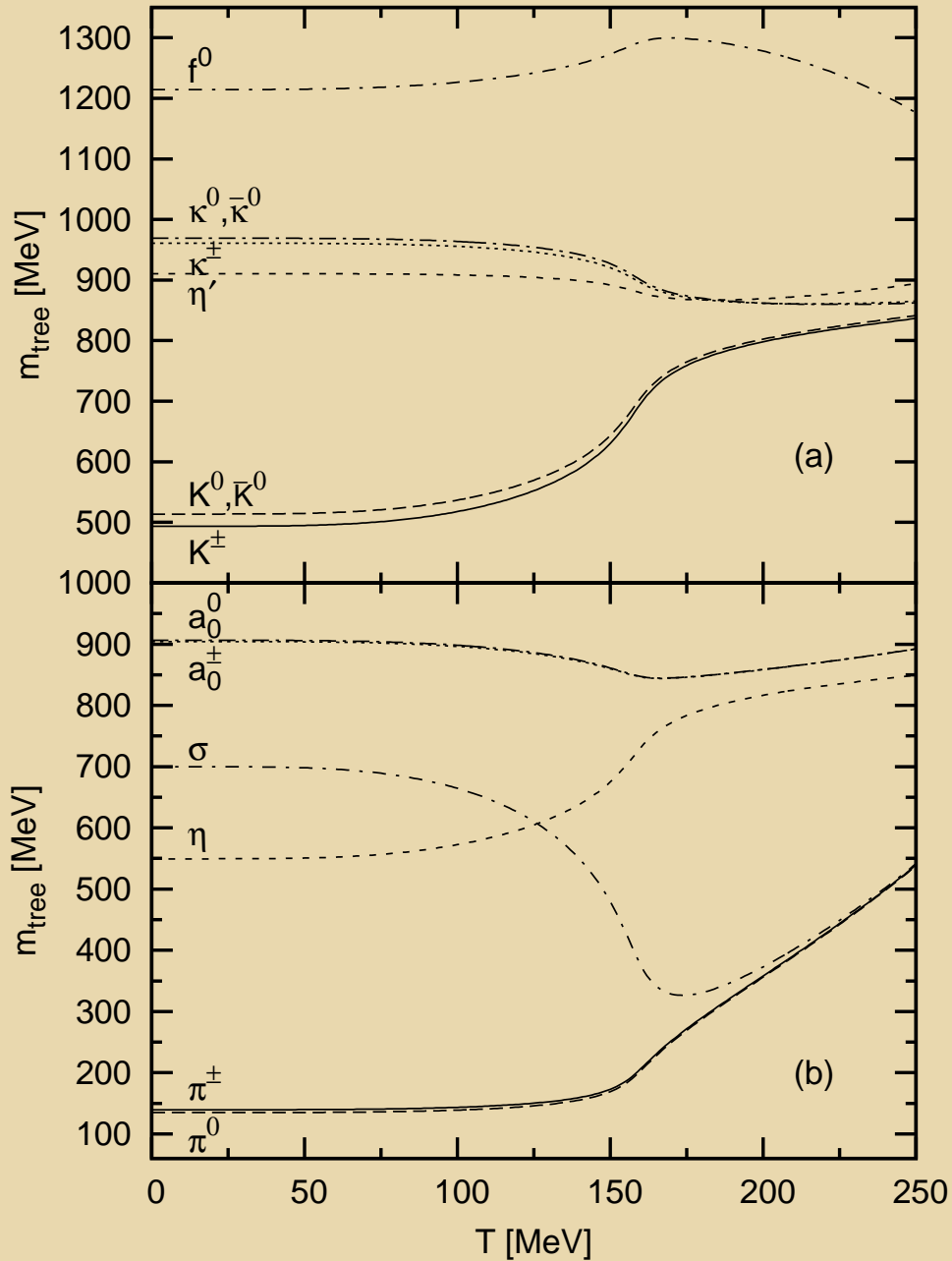
On the right Fig.:  $\mu_I$  dependence at a given  $\mu_B$

Increasing of either  $\mu_B$  or  $\mu_I$   $\longrightarrow$  influence of  $v_3$  becomes stronger

CEP at  $\mu_I = 0$ :  $T_{\text{CEP}} = 63.08 \text{ MeV}$ ,  $\mu_{B,\text{CEP}} = 960.8 \text{ MeV}$   $\longrightarrow$  large diff. to case  $v_3 = 0$

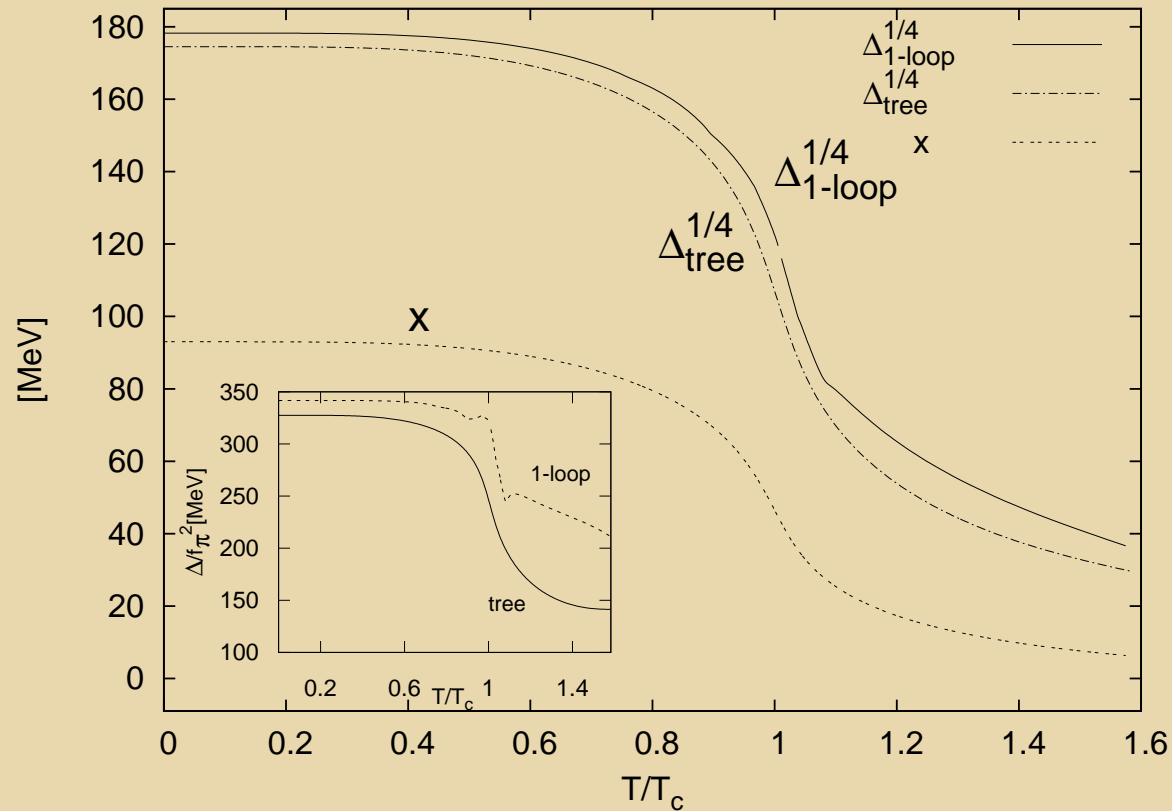
Reason:  $x$  and  $v_3$  related  $\longrightarrow$  common transition point

# Tree-level and 1-loop pole masses





# Estimation of the topological susceptibility



$$\Delta = \frac{1}{6}(m_\eta^2 + m_{\eta'}^2 - 2m_K^2)f_\pi^2$$

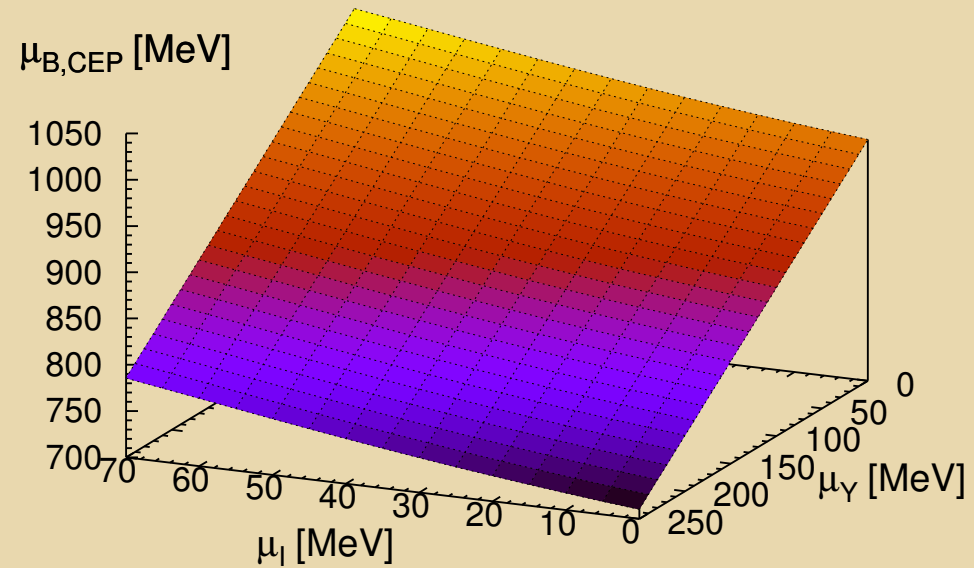
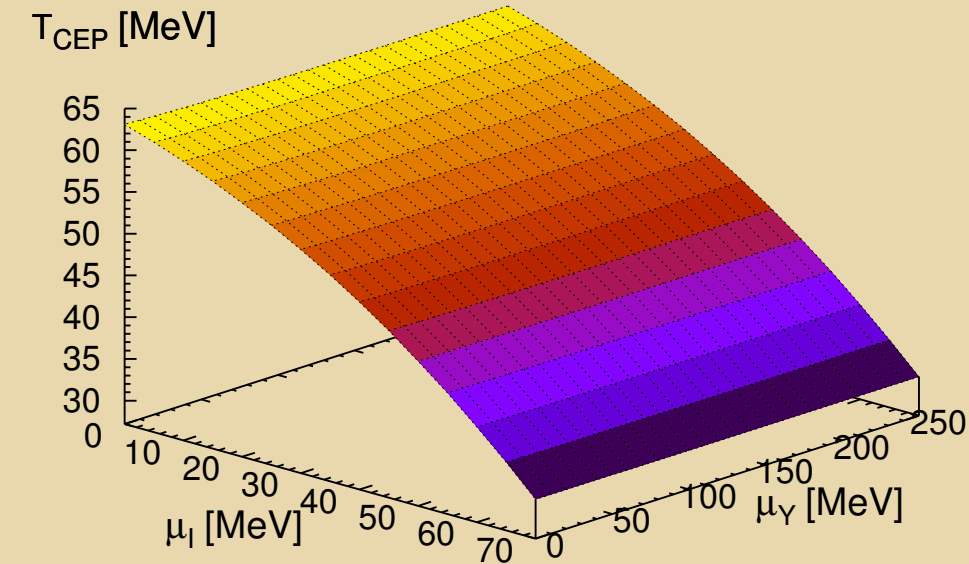
This is an estimation of  $\chi_T(T)$  the **topological susceptibility** through

Witten-Veneziano formula:  $\frac{2N_f}{f_\pi^2}\chi_T = m_\eta^2 + m_{\eta'}^2 - 2m_K^2$

→ Connection with the  $U_A(1)$  **anomaly**

Doesn't mean the restoration of  $U_A(1) \rightarrow \chi_T(T)$  is dominated by chiral restoration

## Dependence of the CEP on $\mu_I, \mu_Y$



$T_{\text{CEP}}$  is almost independent of  $\mu_Y$ , but significantly depends on  $\mu_I$

$\mu_{B,\text{CEP}}$  has an almost linear dependence on both chemical potentials  $\mu_I, \mu_Y$

As  $\mu_Y$  is increased the phase transition at  $T = 0$  becomes stronger

## Simple explanation of the influence of $\mu_I, \mu_Y$

**Approximation:** Ideal quantum gas of the quasi-particle degrees of freedom

In the first order region  $\rightarrow$  generalized **Clausius-Clapeyron equations**

Partition function:

$$\ln Z = V \sum_i \gamma_i (2s_i + 1) \int \frac{d^3 p}{(2\pi)^3} \left[ \beta \omega_i + \ln(1 + \alpha_i e^{-\beta(\omega_i - \mu_i)}) + \ln(1 + \alpha_i e^{-\beta(\omega_i + \mu_i)}) \right]$$

Gibbs-Duhem relation:  $dp = s dT + n_B d\mu_B + n_I d\mu_I + n_Y d\mu_Y$

In case of  $dp|_{phase1} = dp|_{phase2}$ :

$$\left. \frac{dT}{d\mu_B} \right|_{\mu_Y, \mu_I} = -\frac{\Delta n_B}{\Delta s}, \quad \left. \frac{dT}{d\mu_Y} \right|_{\mu_B, \mu_I} = -\frac{\Delta n_Y}{\Delta s}, \quad \left. \frac{dT}{d\mu_I} \right|_{\mu_B, \mu_Y} = -\frac{\Delta n_I}{\Delta s},$$

$$\left. \frac{d\mu_B}{d\mu_Y} \right|_{T, \mu_I} = -\frac{\Delta n_Y}{\Delta n_B}, \quad \left. \frac{d\mu_B}{d\mu_I} \right|_{T, \mu_Y} = -\frac{\Delta n_I}{\Delta n_B}$$

Obtained relations:  $\Delta n_B, \Delta n_Y, \Delta s > 0, \Delta n_I < 0$

$$\Delta n_B \approx \Delta n_Y, \Delta s > \Delta n_B, \Delta s > |\Delta n_I|$$

## Conclusions and outlook

- The 2<sup>nd</sup> order surface was determined in the  $m_\pi - m_K - \mu_B$  space using ChPT to obtain the  $m_\pi, m_K$  dependence of the couplings and of the constituent quark masses.
- The CEP is robustly predicted and at the physical point of the mass-plane was located at:  $T_{CEP} = 74.83 \text{ MeV}$   $\mu_{B,CEP} = 895.38 \text{ MeV}$ .
- The dependence of the  $\mu_B$  on the width of the susceptibility was investigated.
- $\mu_I$  dependence of different pole masses were obtained.
- The temperature dependence of the topological susceptibility was estimated.
- Effects of isospin and hyper chemical potential on the CEP was investigated.  $T_{CEP} = 63.08 \text{ MeV}$   $\mu_{B,CEP} = 960.8 \text{ MeV}$  at  $\mu_I = 0$  ( $v_3 \neq 0$  at  $T = 0$ ).
- A simple ideal gas model was established, which could explain the shifts of the CEP due to  $\mu_I, \mu_Y$
- **Possible continuation:** Pion condensate, inclusion of the Polyakov-loop